Available online at www.sciencedirect.com
SCIENCE DIRECT®
Optical Materials 27 (2005) 1576–1582
OPTICAL Materials
www.elsevier.com/locate/optmat

Spectroscopic properties of Yb^{3+} doped $PbO–Bi_2O_3–Ga_2O_3$ glasses for IR laser applications

L.R.P. Kassab [a,*], M.E. Fukumoto [b], V.D.D. Cacho [b], N.U. Wetter [c], N.I. Morimoto [b]

[a] *Laboratòrio de Vidros e Datação, Faculdade de Tecnologia de São Paulo, Centro Estadual de Educação Tecnológica Paula Souza/UNESP, Praça Coronel Fernando Prestes 30, CEP 01124-060 São Paulo, SP, Brazil*
[b] *Laboratório de Sistemas Integrados, Departamento de Sistemas Eletrônicos, Escola Politécnica, Universidade de São Paulo, São Paulo, SP, Brazil*
[c] *Centro de Lasers e Aplicações, Instituto de Pesquisas Energéticas e Nucleares, São Paulo, SP, Brazil*

Received 15 November 2004; accepted 11 April 2005
Available online 1 June 2005

Abstract

$PbO–Bi_2O_3–Ga_2O_3$ glasses doped with different concentrations of Yb^{3+} are presented. The spectroscopic properties and laser parameters are calculated and a comparison between different results obtained when calculating the Yb^{3+} emission cross-section with the reciprocity method and with the Fuchtbauer–Ladenburg formula is presented. The behavior of the near-infrared luminescence is described theoretically by a rate equation and compared with the experimental results. This host doped with Yb^{3+} is a promising material for laser action at 1019 nm, with properties similar to other known glasses used as active laser media; the emission cross-section of $1.1 \times 10^{-20}\,cm^2$, the high absorption cross-section (of $2.0 \times 10^{-20}\,cm^2$) and a minimum pump intensity of $2.4\,kW/cm^2$ are interesting properties for short pulse generation.

PACS: 42.70.a; 42.70.km

Keywords: Glasses; Ytterbium; Fluorescence

1. Introduction

The discovery of heavy metal oxide glasses [1–3] has attracted interest for photonics and optoelectronic applications because of their optical properties such as high refractive indices and infrared transmittance up to 8 μm. Because of the high refractive index, contributions of third and fifth order susceptibilities were observed in $PbO–Bi_2O_3–Ga_2O_3$ glasses produced at the Laboratory of Glasses and Datation and indicate that these glasses may be useful as efficient optical limiters in the nanosecond regime [4]. Also, the reduced phonon energy ($500\,cm^{-1}$), comparable to ZBLA glasses [5], provides the possibility to develop more efficient lasers and fiber optic amplifiers at longer wavelengths than available from other glasses (silicate, borate, germanate, phosphate and tellurite glasses have phonon energies, higher than $700\,cm^{-1}$) [6]. The broad emission bands of Yb^{3+} doped glasses are important to generate tunable laser emission, as well as ultra-short pulses. The location of the absorption band (900–1000 nm) is suited for pumping with InGaAs laser diodes. The literature recently presented the optical properties of Er^{3+}, Nd^{3+}, Tm^{3+}, Pr^{3+} and Dy^{3+} [7–9] in glasses based on $PbO–Bi_2O_3–Ga_2O_3$. In this work Yb^{3+} spectroscopic properties are investigated in a ternary composition of $PbO–Bi_2O_3–Ga_2O_3$ glasses (BPG), suggested by Dumbaugh [1]. The laser parameters (I_{min}, I_{sat} and β_{min}) are calculated and the effect of radiation trapping is discussed

* Corresponding author. Fax: +55 11 33267611.
E-mail address: kassablm@osite.com.br (L.R.P. Kassab).

0925-3467/$ - see front matter © 2005 Elsevier B.V. All rights reserved.
doi:10.1016/j.optmat.2005.04.006

[10]. The rate equation is used to compare the theoretical near-infrared luminescence with the experimental results. To the best of our knowledge there are no similar studies related to PbO–Bi_2O_3–Ga_2O_3 glasses doped with Yb^{3+}.

2. Experimental

Batches of 12 g were prepared by mixing high purity (99.99%) elements. Different concentrations of Yb_2O_3 shown in Table 1 in wt% (the ionic concentrations are also presented) and representing the initial ones for the synthesis, were added to the ternary lead bismuth gallium composition (46.0PbO–42.0Bi_2O_3–12.0Ga_2O_3 (wt%)) or BPG as suggested by Dumbaugh [1]. The powders were melted in high purity platinum crucibles at 1000 °C, for 1 h, quenched in air inside heated brass molds, annealed for 3 h at 300 °C (considering the transition temperature, T_g, of 324 °C) and then cooled to room temperature inside the furnace. The melts of these ternary systems are very reactive and corrosive and this makes the choice of the crucible material a problem. However platinum and gold crucibles seem to show the best resistance and also give the best infrared transmission. Contamination by platinum shifts the transmission edge to longer wavelengths [1]. The intrinsic color of the glass is yellow because of the combination of bismuth and lead. The final color is a result of the combination of this intrinsic yellow and eventual contamination by the crucible. Results of the transition (T_g) and crystallization (T_c = 393 °C) temperatures were obtained using the DTA technique. The samples produced have a red coloration and are stable against crystallization as $T_g - T_c$ = 69 °C, in agreement with previous reports [11]; the quantity ($T_g - T_c$) has been frequently used as a measure of glass stability and its value has to be as large as possible [11]. Energy dispersive X-ray spectroscopy (EDS) is a chemical microanalysis technique that was performed in conjunction with a scanning electron microscope (SEM) to evaluate the presence of impurities and the complete melting of the rare-earths. X-ray measurements were performed to confirm the amorphous structure. Refraction index of 2.3 was measured at 1019 nm. Finally the samples were polished for absorption, emission and lifetime measurements. For Yb^{3+} concentrations higher than 2.1×10^{20} ions/cm^3 we observed a lack of transparency indicating the solubility limit of Yb_2O_3 in this heavy metal oxide glass under the melting condition employed. The absorption spectra were measured at room temperature from 800 nm to 1300 nm, using a Spectrometer (Carry 500). Emission measurements were performed by optically pumping the samples with an InGaAs laser diode (Optopower A020) at 980 nm (FWHM of 2.2 nm). The emission was analyzed with a monochrometer and detected by a Ge detector. In order to minimize reabsorption due to radiation trapping [10] the samples were excited closely to their edges. Errors in these measurements are estimated to be ±5%, based on the signal to noise ratio. The lifetimes of the excited Yb^{3+} ions were measured using pulsed laser excitation (4 ns) from an Optical Parametric Oscillator pumped by a frequency doubled Nd:YAG laser (Quantel) and a InSb detector with appropriate filter. The wavelength of excitation for lifetime measurements was of 980 nm. Errors are estimated to be ±5%. Because of the spectral overlap of the emission and absorption bands of Yb^{3+}, radiation trapping [10] makes the measured lifetime longer than that of a single isolated ion. To reduce the effect of the radiation trapping due to self absorption, the samples used in the lifetime measurements had thickness of 0.3 mm [12]. The samples have good mechanical resistance under high-brightness diode laser pumping: at 7.5 W of cw diode pump power there was no visible fracture in the samples, even in the absence of cooling.

Table 1
Spectroscopic properties and the laser parameter (I_{min}) of BPG glasses doped with different concentrations of Yb^{3+}

Yb^{3+} ($\times 10^{20}$ ions/cm^3)	Yb_2O_3 (wt%)	τ_f (±5% ms)	I_{min} (kW/cm^2)
0.11	0.05	0.31	2.6
0.21	0.10	0.34	2.6
0.53	0.25	0.35	2.4
1.60	0.75	0.36	2.9
2.10	1.00	0.37	3.0

3. Results

Fig. 1 shows the transmission spectrum in the infrared region in which we can see the cutoff wavelength of about 8 μm; the presence of the OH^- band at 3.25 μm can also be observed. Fig. 2 shows the absorption spectrum of the sample doped with ytterbium and the transmission edge in the visible region at about 570 nm.

The two most usual methods to obtain the emission cross-section of the Yb^{3+}: $^2F_{7/2} \rightarrow {}^2F_{5/2}$ transition are the reciprocity method (RE) [13] and the Fuchtbauer–Ladenburg (F–L) formula [14]. The latter requires knowledge of the spontaneous emission probability and of the emission line shape as follows:

$$A_R = \frac{8\pi c n^2 (2J'+1)}{\lambda_p^4 (2J+1)\rho} \int k(\lambda) d\lambda \quad (1)$$

$$\sigma_{em}(\lambda) = \frac{\lambda^4 g(\lambda) A_R}{8\pi n^2 c} \quad (2)$$

where A_R represents the radiative rate from the $^2F_{5/2}$ energy level, c the velocity of light, n the refractive index,

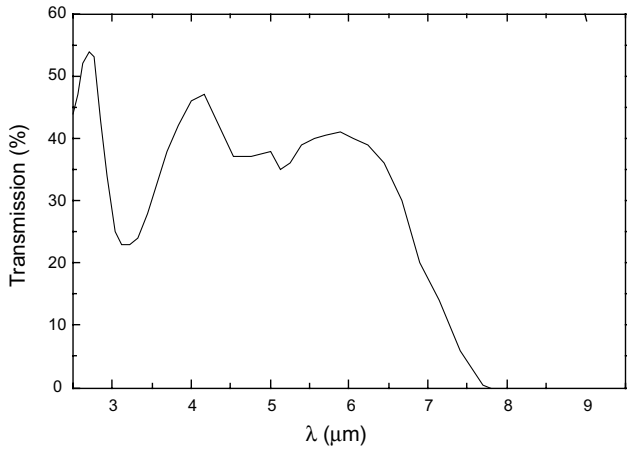

Fig. 1. Transmission spectrum of BPG glass doped with 0.53×10^{20} ions/cm^{3+} of Yb^{3+} (2.5 mm thickness).

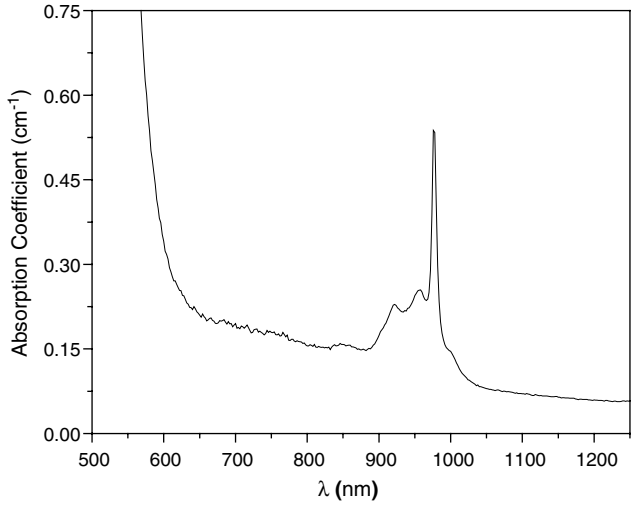

Fig. 2. Absorption spectrum of BPG glass doped with 0.53×10^{20} ions/cm^3 of Yb^{3+} (2.5 mm thickness).

λ_p the absorption peak wavelength (978 nm), ρ the concentration of Yb^{3+} ions, $k(\lambda)$ the absorption coefficient, J and J' the total momentum for the upper and lower levels and $g(\lambda)$ the normalized line shape function of the measured fluorescence transition of Yb^{3+}. However, accurate experimental determination of the fluorescence spectrum, easily affected by radiation trapping, is normally difficult. The reciprocity method does not include radiation trapping because it is obtained from the absorption cross-section spectrum (σ_{abs}) using the relation given by [13]:

$$\sigma_{em}(\lambda) = \sigma_{abs}(\lambda)\frac{Z_l}{Z_u}\exp\left(\frac{E_{zl} - hc\lambda^{-1}}{kT}\right) \quad (3)$$

where k and E_{zl} represent the Boltzmann constant and the zero line energy that is defined as the energy separation between the lowest components of the upper and lower states, respectively. In the high temperature limit, the ratio of the partition functions (Z_l/Z_u) simply becomes the degeneracy weighting of the two states. Fig. 3 shows the emission and absorption cross-sections for Yb^{3+} doped BPG glasses with 0.3 mm thickness; a high absorption cross-section of 2.0×10^{-20} cm^2 is observed (FWHM of 10 nm). The emission cross-sections are calculated using the reciprocity method (RE) and the Fuchtbauer–Ladenburg (F–L) formula. Based on cumulative errors associated with the spectra, concentration and energy level assignments, we estimate that the emission cross-sections are accurate to ±18% and ±9%, respectively, considering, F–L and RE calculations. Normally the discrepancies of the emission cross-sections calculated by RE and F–L are mainly due to radiation trapping [10]. Using F–L equation to calculate the spontaneous emission probability, assuming for the emission cross-section the results obtained from the reciprocity method we confirmed the radiative lifetime ($\tau_R = 1/A_R = 0.3$ ms) obtained from Eq. (1) and the match between RE and F–L calculations. Table 1 shows some of the spectroscopic properties; τ_f is the fluorescence lifetime obtained by fitting the measured lifetime to a single exponential function (the changes of the fluorescence lifetime are of the order of the experimental errors of ±5%; these values are also in agreement with the radiative lifetime of 0.3 ms) and I_{min} is the minimum pump intensity, a laser parameter that is a measure of the ease of pumping in order to get laser action [15]:

$$I_{min} = \beta_{min} I_{sat} \quad (4)$$

where

$$\beta_{min} = \frac{\sigma_{abs}(\lambda_{ext})}{\sigma_{em}(\lambda_{ext}) + \sigma_{abs}(\lambda_{ext})} \quad (5)$$

$$I_{sat} = \frac{hc}{\lambda_p \tau_f \sigma_{abs}(\lambda_p)}. \quad (6)$$

In the equations above, $\sigma_{abs}(\lambda_p)$ is the absorption cross-section at the absorption peak wavelength (λ_p = 978 nm), $\sigma_{em}(\lambda_{ext})$ and $\sigma_{abs}(\lambda_{ext})$ are, respectively, the emission and the absorption cross-sections at the extraction wavelength (λ_{ext} = 1019 nm). At this wavelength I_{min} assumes the lowest value. We remark that at 1019 nm the absorption cross-section is two times smaller than at 1005 nm (this is the wavelength that corresponds to the emission cross-section of the secondary peak). Concerning the emission cross-sections, the differences between their values, at 1019 nm and 1005 nm, are within the experimental errors. Therefore, 1019 nm is chosen as the extraction wavelength for the calculation of I_{min}. I_{sat} is the pump saturation intensity that characterizes the pumping dynamics and the β_{min} parameter is defined as the minimum fraction of Yb ions that must be excited to balance the gain exactly with the ground-state absorption at λ_{ext}.

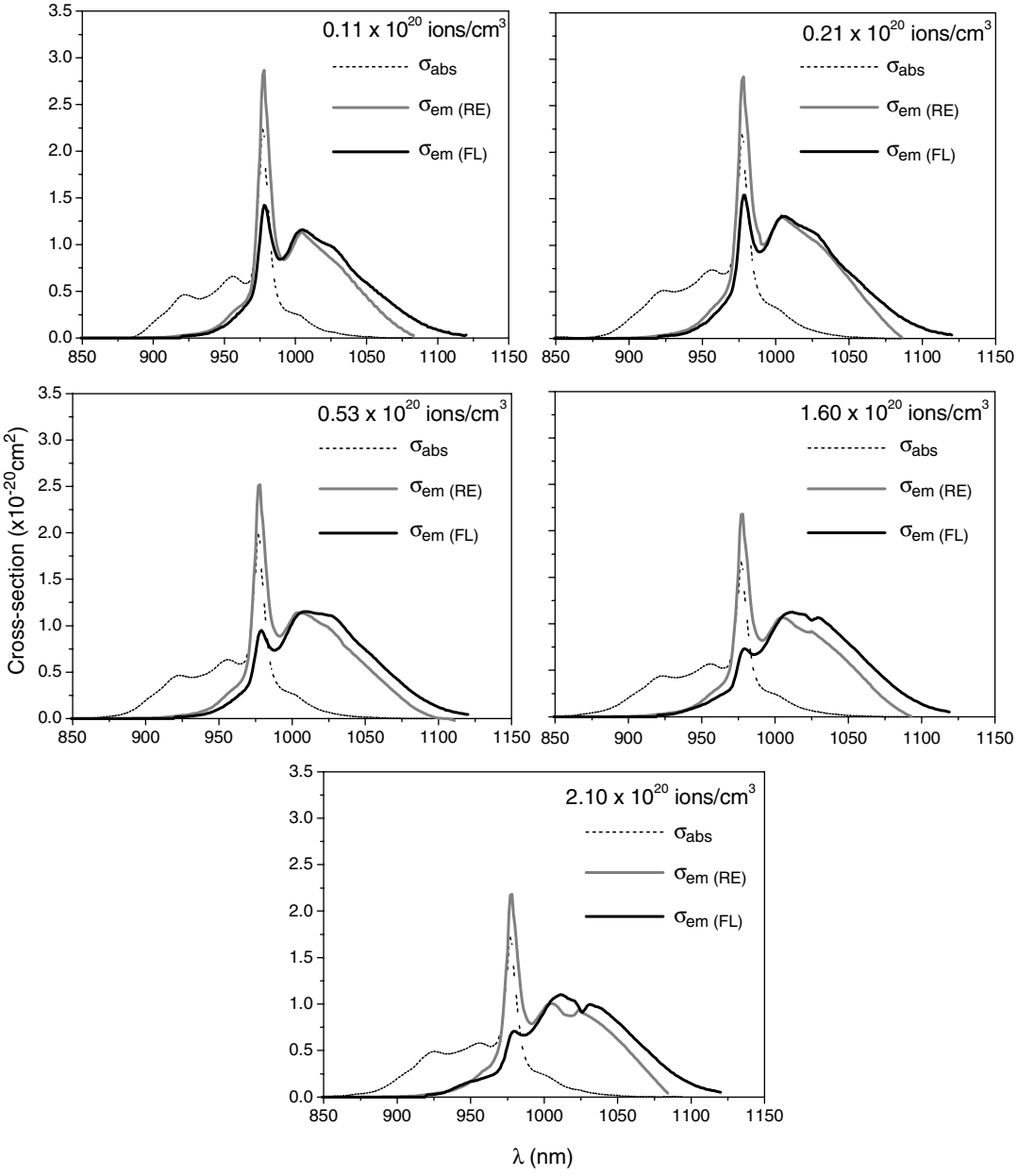

Fig. 3. Absorption and emission cross-section spectra (calculated with RE and F–L methods) for BPG glasses doped with different concentrations of Yb^{3+}.

Zhang and Hu [16] proposed that radiation trapping can be evaluated by the parameter rtc (radiation trapping coefficient) also used recently by Bell et al. [17] and defined as follows: $((\sigma_{ems}/\sigma_{emp})_{FL} - (\sigma_{ems}/\sigma_{emp})_{RE})/(\sigma_{ems}/\sigma_{emp})_{RE}$. Here σ_{emp} and σ_{ems} are the emission cross-sections at the primary (978 nm) and secondary (1005 nm) peaks, respectively, represented in Fig. 3. The results of rtc calculations are presented in Table 2. The radiation trapping tends to increase with the increase of the Yb^{3+} concentration and occurs even for small doping levels. Similar results for the rtc parameter were reported in Yb tetraphosphate glasses [16] and in phosphate glasses [17]. We observe from Table 2 that $(\sigma_{emp})_{RE}$ is larger than $(\sigma_{emp})_{FL}$. Considering the ratio of the secondary to primary peak, we obtain $(\sigma_{ems}/\sigma_{emp})_{FL} > (\sigma_{ems}/\sigma_{emp})_{RE}$ and $(\sigma_{ems}/\sigma_{emp})_{RE}$ remains approximately constant whereas $(\sigma_{ems}/\sigma_{emp})_{FL}$ increases with increasing Yb^{3+} concentration. The best agreement between RE and F–L methods is obtained at the secondary peak. These results can be attributed to radiation trapping, as reported by Zhang and Hu [16], in Yb tetraphosphate glasses. With increasing Yb^{3+} concentration the fluorescence trapping increases and the fluorescence peak at 978 nm is reabsorbed, whereas the secondary

Table 2
Comparison between RE and F–L calculations of the Yb^{3+} emission cross-sections of BPG glasses

Yb^{3+} (10^{20} ions/cm^3)	σ_{emp} ($\times10^{-20}$ cm^2)		σ_{ems} ($\times10^{-20}$ cm^2)		$\sigma_{ems}/\sigma_{emp}$		rtc
	RE	FL	RE	FL	RE	FL	
0.11	2.9	1.4	1.1	1.1	0.4	0.8	1.0
0.21	2.8	1.5	1.2	1.2	0.5	0.9	0.8
0.53	2.5	0.9	1.1	1.1	0.4	1.2	2.0
1.60	2.2	0.7	1.1	1.1	0.5	1.6	2.2
2.10	2.2	0.7	1.0	1.1	0.5	1.5	2.0

rtc = $((\sigma_{ems}/\sigma_{emp})_{FL} - (\sigma_{ems}/\sigma_{emp})_{RE})/(\sigma_{ems}/\sigma_{emp})_{RE}$ (radiation trapping coefficient).

peak increases, leading to the increase of $(\sigma_{ems}/\sigma_{emp})_{FL}$. This explains the disagreement (Fig. 3), between the two methods.

The dependence of the cooperative [18] and near-infrared intensities on Yb^{3+} concentration can be described theoretically by a rate equation that includes the nonradiative losses, as done in Auzel et al. [19] and also in Bell et al. [17]:

$$\frac{dN_2}{dt} = RN_1 - A_R N_2 - XN_2^2 - W_{nr}N_2 \quad (7)$$

where N_i ($i = 1, 2$) stands for the populations of levels 1 and 2, which correspond to the $^2F_{7/2}$ and $^2F_{5/2}$ energy levels, respectively. The total Yb^{3+} concentration is $N_1 + N_2 = N_{Yb}$, A_R is the radiative rate from the $^2F_{5/2}$ level, and X is the cooperative rate. Eq. (7) means that the population of the $^2F_{5/2}$ level is increased by a pumping term RN_1 that depends on the laser intensity (I) according to $R = \sigma_{abs}I/h\nu$, where R is the pumping rate and σ_{abs} is the absorption cross-section at the pumping energy $h\nu$. $W_{nr}N_2$ accounts for nonradiative losses and XN_2^2 indicates the loss of population of the $^2F_{5/2}$ level by the creation of Yb^{3+} pairs [17]. From Eq. (7) we can determine the intensity of the luminescence in the visible and near-infrared regions because these emissions depend on the N_2 population. We determine N_2 considering the sample under low excitation density (N_1 can be approximated to the total concentration N_{Yb}) and in the stationary condition ($dN_2/dt = 0$).

$$N_2 = \frac{RN_{Yb}}{A_R + W_{nr}} = RN_{Yb}\tau_f. \quad (8)$$

In Eq. (8), τ_f is the experimental lifetime of the $^2F_{5/2}$ level. The cooperative effect was also neglected because it contributes very little for emptying the state $^2F_{5/2}$ when compared to $A_R N_2$. This cooperative effect is responsible for the emission at about 500 nm, and was not observed in this glass. From Eq. (8) it follows that:

$$N_2' = \frac{N_2}{R} = N_{Yb}\tau_f. \quad (9)$$

The intensity of the near-infrared emission is proportional to $N_2' = N_2/R$. Fig. 4 shows the luminescence (N_2') in the near-infrared as predicted by the rate equation (Eq. (9)) and the experimental results (I_{IR}) obtained from the emission measurements (I_{IR} represents the intensity of the measured luminescence at the secondary peak emission).

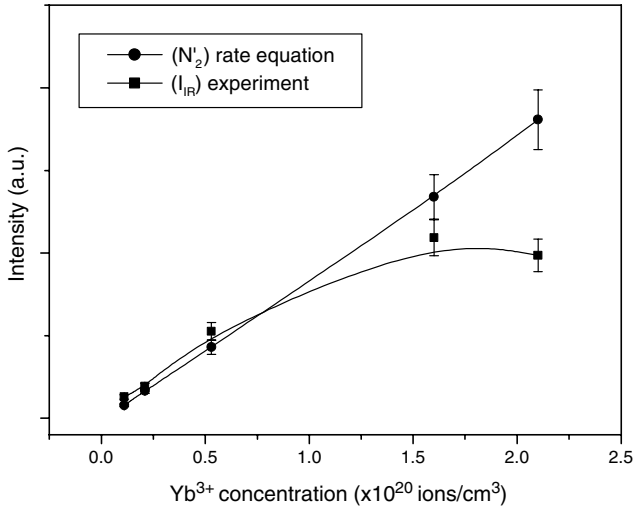

Fig. 4. Experimental (I_{IR}) and theoretical (N_2') near-infrared emission.

4. Discussion

The absorption measurements indicate the incorporation of Yb^{3+}, because of the maximum absorption at 978 nm and the two weaker absorptions with maxima at 920 nm and 950 nm. These bands correspond to the transition from the ground state $^2F_{7/2}$ to the excited state $^2F_{5/2}$ of Yb^{3+}, that splits into three levels in glasses; therefore, the absorption spectrum may be resolved into three broad bands (for phosphate glasses the spectrum consists of four bands) [20]. The large transmission window provides the possibility to develop lasers at longer wavelength and the high absorption cross-section at the pump wavelength (978 nm) is adequate for efficient diode pumping.

From the point of view of laser operation, it is generally desirable for the emission cross-section to be as large as possible to provide for greater gain, for the fluorescence lifetime to be long in order to permit high inversion densities and for the absorption cross-section at the

Table 3
Spectroscopic properties and the I_{min} parameter of Yb^{3+} doped laser glasses and BPG glass (doped with 0.53×10^{20} ions/cm^3 of Yb^{3+})

Materials		System	$\sigma_{em}(\lambda_{ext})$ ($\times 10^{-20}$ cm^2)	λ_{ext} (nm)	τ_f (ms)	I_{min} (kW/cm^2)	σ_{abs} (λ_p) ($\times 10^{-20}$ cm^2)
QX	[21]	Phosphate	0.70	1018	2.00	1.8	0.50
ADY	[22]	Aluminate	1.03	1020	1.58	1.1	0.70
LY	[23]	Silicate	0.80	1028	1.68	2.0	0.55
PN	[24]	Phosphate	1.35	1035	1.36	0.6	1.00
PNK	[24]	Phosphate	1.08	1016	2.00	1.3	0.68
FP	[23]	Fluorophosphate	0.50	1020	1.20	0.8	0.43
YTG	[21]	Tellurite	2.35	1024	0.90	0.8	1.64
BPG		Heavy metal oxide	1.1	1019	0.34	2.4	2.00

pump wavelength to be as large as possible to allow for efficient diode pumping. These considerations lead the laser parameters (I_{min}, I_{sat} and β_{min}) with low values. An efficient host for laser operation should also incorporate a high concentration of the trivalent rare-earth ion as the laser gain is proportional to the doping concentration. Important spectroscopic properties and the I_{min} values of different laser glasses [21–24] are compared in Table 3 to the BPG samples (Yb^{3+} doping level: 0.53×10^{20} ions/cm^3). From Table 3 we observe that Yb^{3+} doped BPG glasses have a larger absorption cross-section at 978 nm and that the laser parameter I_{min} is within the acceptable limits, always less than 4.5 kW/cm^2 [15], which can be achieved with standard diode pumping. BPG has, at 1019 nm, an emission cross-section larger than Yb:QX (a commercial phosphate laser glass from Kigre Incorp) [21] and is comparable to ADY [22] and PNK glasses [24]; the fluorescence lifetime is, however, the smallest, but is in good agreement with the radiative lifetime.

The behavior of the near-infrared luminescence, as a function of Yb^{3+} concentration is described theoretically (N_2') and compared with the experimental results (I_{IR}). We observe a good agreement between the experimental and theoretical results up to 0.53×10^{-20} cm^2, considering the errors (±5% for the experimental and ±10% for the theoretical results); a tendency of decrease, for the experimental results, is observed starting at 1.6×10^{-20} ions/cm^3 of Yb^{3+} and may be attributed to the nonradiative processes caused by interaction between Yb^{3+} ions and host impurities (using EDS and SEM techniques, from 1.6×10^{-20} ions/cm^3 of Yb^{3+}we observe the appearance of clusters) that explains the slight decrease of the absorption cross-section with the increase of Yb^{3+} [16,17].

5. Conclusion

BPG glasses doped with different concentrations of Yb^{3+} are presented for IR laser applications. They have spectroscopic properties suitable for laser action at the extraction wavelength of 1019 nm and comparable to other known laser glasses developed recently. For a doping level of 0.53×10^{20} ions/cm^3 the absorption cross-section at 978 nm is 2.0×10^{-20} cm^2, the emission cross-section at 1019 nm is 1.1×10^{-20} cm^2 and the possibility of getting laser action is revealed by $I_{min} = 2.4$ kW/cm^2. These features put BPG glasses doped with Yb^{3+} among other promising materials for short pulse laser generation.

Acknowledgements

We would like to thank for the support from CAPES, FAPESP, CNPq and also Dr. Samuel de Oliveira Leite for the discussions on the rate equation.

References

[1] W.R. Dumbaugh, Physics and Chemistry of Glasses 27 (1986) 119.
[2] W.R. Dumbaugh, Physics and Chemistry of Glasses 19 (1978) 121.
[3] M.M. Wierzbicki, J.E. Shelby, Physics and Chemistry of Glasses 36 (3) (1995) 150.
[4] E.O. Silva, E.L.F. Filho, C.B. de Araújo, L.R.P. Kassab, XXVII ENFMC, Poços de Caldas, MG, Brazil, May 2004.
[5] Y.G. Choi, J. Heo, Journal of Non-Crystalline Solids 217 (1997) 199.
[6] D. Lezal, J. Pedlikova, P. Kostka, J. Bludska, M. Poulain, J. Zavadil, Journal of Non-Crystalline Solids 284 (2001) 288.
[7] D.J. Coleman, S.D. Jackson, P. Golding, T.A. King, Journal of the Optical Society of America B 19 (2002) 2927.
[8] L.R.P. Kassab, S.H. Tatumi, C.M.P. Mendes, L.C. Courrol, N.U. Wetter, Optics Express 6 (2000) 104.
[9] J. Heo, Y.B. Shin, J.N. Jang, Applied Optics 21 (1995) 4284.
[10] M.J. Weber, J.E. Lynch, D.H. Blackburn, D.J. Cronin, IEE Journal of Quantum Electron 19 (1983) 1600.
[11] L. Le Neindre, S. Jiang, B.C. Hwang, T. Luo, J. Watson, N. Peyghambarian, Journal of Non-Crystalline Solids 255 (1999) 97.
[12] S. Dai, J. Yang, L. Wen, L. Hu, Z. Jiang, Journal of Luminescence 104 (2003) 55.
[13] D.E. McCumber, Physical Review A954 (1964) 136.
[14] C. Li, Y. Guyot, C. Linares, R. Moncorgé, M.F. Joubert, Proceedings on Advanced Solid-State Lasers 5 (1993) 91.
[15] L.D. Deloach, S.A. Payne, L. Smith, W.L. Kway, W.F. Krupke, Journal of the Optical Society of America B 11 (1994) 269.
[16] L. Zhang, H. Hu, Journal of Non-Crystalline Solids 292 (2001) 108.

[17] M.J.V. Bell, W.G. Quirino, S.L. Oliveira, D.F. deSousa, L.A.O. Nunes, Journal of Physics: Condensed Matter 15 (2003) 4877.
[18] E. Nakazawa, S. Shionoya, Physics Review Letters 25 (1970) 1710.
[19] F. Auzel, P.H. Goldner, D. Meichenin, F. Pelle, Journal of Luminescence 71 (1997) 137.
[20] H. Takebe, T. Murata, K. Morinaga, Journal of American Society 79 (1996) 681.
[21] R. Koch, U. Griebner, H. Schonnagel, S. Jiang, Optics Communication 134 (1997) 175.
[22] C. Jiang, H. Liu, Q. Zeng, X. Tang, F. Gan, Journal of Chemistry and Physics of Solids 61 (2000) 1217.
[23] V. Petrov, U. Griebner, D. Ehrt, W. Seeber, Optics Letters 22 (1997) 408.
[24] C. Jiang, F. Gan, J. Zhang, P. Deng, G. Huang, Materials Letters 41 (1999) 209.